# *One-Dimensional Inverse Scattering Problem in Acoustics*

**Demetrios Gerogiannis, Sofianos Antoniou Sofianos, Isaac Elias Lagaris & Georgios Antomiou Evangelakis**

**Brazilian Journal of Physics**

ISSN 0103-9733
Volume 41
Combined 4-6

Braz J Phys (2011) 41:248-257
DOI 10.1007/s13538-011-0039-9


Springer

Braz J Phys (2011) 41:248–257
DOI 10.1007/s13538-011-0039-9

GENERAL AND APPLIED PHYSICS

# One-Dimensional Inverse Scattering Problem in Acoustics

**Demetrios Gerogiannis · Sofianos Antoniou Sofianos · Isaac Elias Lagaris · Georgios Antomiou Evangelakis**

Received: 22 July 2011 / Published online: 14 September 2011


**Abstract** We are concerned with the inverse scattering problem (ISP) in acoustics within the Marchenko inversion scheme. The quantum ISP is first discussed and applied in order to exhibit certain characteristics and application prospects of the method which could be useful in extending it to classical systems. We then consider the ISP in acoustics by assuming plane waves propagating in an elastic, isotropic, and linear medium. The wave equation is first transformed into a Schrödinger-like equation which can be brought into the Marchenko integral equation for the associated nonlocal kernel the solution of which provides us the full information of the underlying reflective profile. We apply the method in several model problems where the reflection coefficient of the multi-layer reflective medium is used as input to the ISP and in all cases we obtain excellent reproduction of the original structure of the scatterer. We then applied the inverse scattering scheme to construct profiles with certain predetermined reflection and transmission characteristics.

**Keywords** Inverse scattering theory · Acoustics

D. Gerogiannis · I. E. Lagaris
Department of Computer Science, University of Ioannina, 451 10, Ioannina, Greece

S. A. Sofianos (✉) · I. E. Lagaris
Physics Department, University of South Africa, Pretoria 0003, South Africa
e-mail: sofiasa@science.unisa.ac.za

G. A. Evangelakis
Department of Physics, University of Ioannina, 451 10, Ioannina, Greece

## 1 Introduction

In scattering theory, one considers the effects a medium has on an incident wave and how it scatters. In quantum mechanical systems, the whole process is described by the Schrödinger equation and from the knowledge of the potential one gets from its solution the wave function which contains the full information for the scattering. In classical systems one has instead profiles and the usual classical wave equation. The solution of the latter depends on the characteristics of the scatterer and provides us the dynamics of the scattering. The above process, in both the quantum and classical physics, is usually called the *direct* scattering problem.

In contrast to the direct problem, in the *inverse* scattering the underlying potential or profile is unknown and one faces the task of reconstructing it from the scattering information available either from an experiment or from some theoretical model. This information includes the knowledge of the reflection coefficient $R(k)$ as well as the bound states information, when present.

The quantum inverse scattering problem (ISP) has afforded numerous theoretical investigations to the extent that it is nowadays textbook material (see, for example, [1–4]). In contrast, applications are limited since its implementation presupposes the knowledge of the reflection coefficient $R(k)$ at all momenta of the incident wave, $k \in (0, \infty)$, and most importantly, the knowledge of the phase of $R(k)$. However, in practice only the modulus of the reflection coefficient, $|R(k)|$, can be measured (this is the famous "phase problem") and thus one has no option but to apply the inversion method based on data extracted from a model problem.

In the present work, we are mainly interested in the classical, one-dimensional, ISP in acoustics in which plane waves are propagated along the $x$-axis coinciding with the direction of a stratified elastic medium. The corresponding classical wave equation for the acoustic wave is first transformed into a Schrödinger-like equation which can be used to extract the reflection coefficient for the effective potential corresponding to the reflective profile(s) which by itself could be useful in Acoustic studies. Furthermore, this equation can be brought into a Marchenko integral equation [1] and, therefore, it can be utilized in the ISP not only to reconstruct the scatterer but also to construct profiles with certain predetermined acoustical characteristics.

The transformation of the classical wave equation into a Marchenko integral equation allows us to take over experiences from the solution of the corresponding quantum mechanical ISP, the theoretical aspects of which are summarized in Section 2. Thereafter, in Section 3.1, the ISP is applied to a quantum system exhibiting strong resonance structure in the reflection coefficient, a behavior usually encountered in classical systems. The inversion method is then employed to demonstrate how to construct quantum systems having predetermined reflection (and transmission) properties. In Section 3.2 the ISP is applied to acoustics by considering three- and five-layer media to show that the method is not only applicable but it could also be very useful in practical applications. Finally, the conclusions drawn from this work are summarized in Section 4.

## 2 Theory

### 2.1 Quantum Systems

In order to elucidate the ISP, let us first summarize the inversion procedure on the half-line for quantum systems. The corresponding Schrödinger equation reads

$$y''(x) + \left(k^2 - V(x)\right) y(x) = 0, \qquad 0 < x < \infty\,, \tag{1}$$

where the potential $V(x)$ is assumed to be real and non-vanishing on a finite interval and the prime denotes the derivative with respect to the variable $x$. The Jost solutions $f_\pm(k,x)$ of (1) are defined by their asymptotic behavior

$$\lim_{x\to\pm\infty} \mathrm{e}^{\mp ikx} f_\pm(k,x) = 1\,. \tag{2}$$

They are given by [2, 9]

$$f_-(k,x) = \begin{cases} \left[\mathrm{e}^{-i\bar{k}x} + R_+(k)\mathrm{e}^{+i\bar{k}x}\right]/T_+(k) & x \to +\infty \\ \mathrm{e}^{-ikx} & x < 0 \end{cases} \tag{3}$$

and

$$f_+(k,x) = \begin{cases} \mathrm{e}^{i\bar{k}x} & x \to +\infty \\ \left[\mathrm{e}^{-ikx} + R_-(k)e^{+ikx}\right]/T_-(k) & x < 0 \end{cases} \tag{4}$$

where $\bar{k} = \sqrt{k^2 - V_s}$ is the wave number in the semi-infinite substrate with potential value $V_s$.

In the following equation, we consider incidence from the left and suppress the corresponding subscripts. We will further assume that $V_s = 0$. An integral equation corresponding to the Jost solution $f(k,x)$ and fully equivalent to (1), is most easily obtained via the Levin representation [2, 3] of $f(k,x)$ which reads

$$f(k,x) = \mathrm{e}^{-ikx} + \int_{-\infty}^{x} M(x,x')\mathrm{e}^{-ikx'}\,\mathrm{d}x'\,. \tag{5}$$

The kernel $M(x,x')$ fulfills the Marchenko integral equation [1]

$$M(x,y) + B(x+y) + \int_{-\infty}^{x} M(x,x')B(x'+y)\,\mathrm{d}x' = 0\,, \quad y < x, \tag{6}$$

where the function $B(z)$ is given by the Fourier transformation of the reflection coefficient

$$B(z) = \frac{1}{2\pi}\int_{-\infty}^{+\infty} R(k)\mathrm{e}^{-ikz}\,\mathrm{d}k + \sum_b A_b\,\mathrm{e}^{\kappa_b z}\,. \tag{7}$$

Here, $\kappa_b^2 = |E_b|$ are the binding energies for the quantum system, $A_b$ the corresponding asymptotic normalization constants while $R(k)$ is the reflection coefficient which for the one-dimensional problem on the half-line can be extracted from the knowledge of the Jost function, i.e., from $f(k,x)|_{x=0}$, and is given by [5]

$$R(k) = \frac{ikf(k,0) - f'(k,0)}{ikf(k,0) + f'(k,0)} \tag{8}$$

where the prime indicates derivative with respect to $x$.

The connection with the experiment is achieved via the reflection coefficient $R(k)$ and the bound state data $\kappa_b$ and $A_b$. Given these data, (6) can be solved and the potential is then readily obtained from

$$V(x) = 2\frac{\mathrm{d}}{\mathrm{d}x}M(x,x)\,, \qquad \text{for } x > 0\,. \tag{9}$$

It is noted that the asymptotic normalization constants can be evaluated from the information of $B(x)$ for negative values of $x$ [6] by noting that (7) can be written as

$$B(x) = \tilde{B}(x) + \sum_b A_b \mathrm{e}^{\kappa_b x}, \tag{10}$$

where $B(x) = 0$ for $x < 0$. Thus

$$\tilde{B}(x_i) = -\sum_{b=1}^{N_b} A_b \mathrm{e}^{\kappa_b x_i} \tag{11}$$

with $x_i < 0$, $i = 1, \cdots, N_b$ and $x_i$ distinct. It is further noted that the construction of the underlying potential from the scattering data (reflection coefficient) in the absence of bound states is unique. When bound states are present, one may construct a family of equivalent potentials which give rise to the same reflection coefficient $R(k)$. Of specific interest is the construction of the so-called super-symmetric partners potentials which, for the one-dimensional case have been discussed in [7, 8].

The above inversion scheme can be used, for example, to design a quantum filter having specific reflection and transmission properties within the momentum interval $k \in [k_a, k_b]$. For this, we may start from a prefabricated profile $V_0(x)$ whose reflection coefficient $R(k)$, and hence its Fourier transform $B(x)$, is known. Assuming now that the reflection coefficient in the interval $k \in [k_a, k_b]$ has another desired new value $R_n(k)$ we may rewrite the new Fourier transform as

$$\tilde{B}_n(x) = \tilde{B}(x) + \frac{1}{2\pi}\int_0^\infty \mathrm{d}k \left[\Delta R^*(k)\mathrm{e}^{ikx} + \Delta R(k)\mathrm{e}^{-ikx}\right] \tag{12}$$

where $\Delta R(k) = -R(k) + R_n(k)$. Using this new Fourier transform, we may obtain the modified profile with the required predetermined characteristics. More details concerning this method can be found in [9].

### 2.2 Classical Systems

Let us consider acoustic waves propagating in an elastic, isotropic, and linear medium. A schematic picture for waves scattered, for example, in a three-layer medium for which the density is $\rho_i$ and the speed of sound is $c_i$, is shown in Fig. 1. The basic equations associated with the propagation of the acoustic wave in a medium characterized by the set of parameters ($\boldsymbol{p}$, $c$, and $\rho$) and ($\Delta\mathbf{p}$, $\boldsymbol{v}$, and $\rho'$) denoting mean values

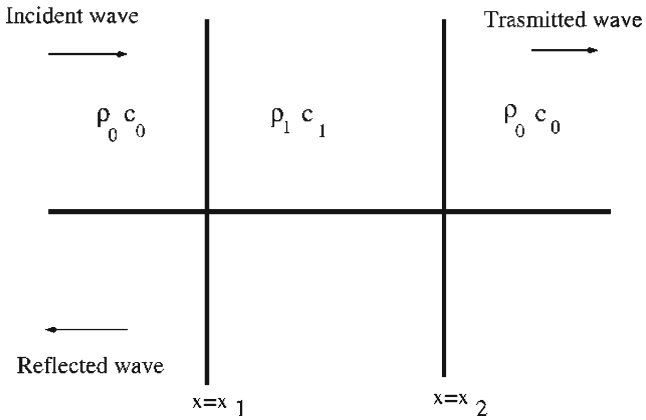


**Fig. 1** Schematic diagram for a three-layer medium

of pressure, speed of sound, density, and their disturbances, are [10]

$$-\nabla \boldsymbol{p} = \rho \frac{\partial}{\partial t}\boldsymbol{v} \tag{13}$$

$$-\rho \nabla \cdot \boldsymbol{v} = \frac{\partial}{\partial t}\rho' \tag{14}$$

$$p = c^2 \rho' \tag{15}$$

where $t$ denotes the time. In the one-dimensional case in which the acoustic wave is propagated in the $x$-direction (subscripts denote the corresponding derivatives with respect to the variable shown), we have

$$-p_x = \rho v_t \tag{16}$$

and

$$-\rho v_x = \rho'_t \tag{17}$$

Substituting $\rho'$ of (15) in (17),

$$-\rho v_x = \frac{p_t}{c^2}, \tag{18}$$

and taking the derivative with respect to $x$ of (16) and $t$ of (18), we obtain the system

$$p_{xx} = -\rho_x v_t - \rho v_{xt}$$
$$\frac{p_{tt}}{c^2} = -\rho_t v_x - \rho v_{xt}$$

or subtracting them and assuming $\rho_t = 0$ (also $c_t = 0$), we obtain

$$p_{xx} - \frac{1}{c^2} p_{tt} = -\rho_x v_t \tag{19}$$

or using (16)

$$p_{xx} - \frac{1}{c^2} p_{tt} = -\left[\ln(\rho)\right]_x p_x. \tag{20}$$

Assuming now that the time dependence is of the form

$$p(x,t) = f(x)\mathrm{e}^{i\omega t} \tag{21}$$

then (20) reduces to

$$f_{xx} + k^2 f = -\left[\ln(\rho)\right]_x f_x \tag{22}$$

where

$$k^2 = \frac{\omega^2}{c^2}\,. \tag{23}$$

For a homogeneous medium, the right hand side vanishes and one simply has the Helmholtz equation

$$f_{xx} + k^2 f = 0\,. \tag{24}$$

Consider now the transformation

$$s(x) = \int_0^x n(x')\,\mathrm{d}x' \tag{25}$$

where $n$ is the index of refraction $n = c_0/c$. The variable $s$ corresponds to the distance traveled in the medium during the same time period as the wave travels from the origin to point $x$. With this transformation, (22) reduces to

$$f_{ss} + \frac{k^2}{a^2} f = -\left[\ln(\rho)\right]_s f_s \tag{26}$$

Noting that $a = \mathrm{d}s/\mathrm{d}x = n = c_0/c$, we obtain

$$f_{ss} + k_0^2 f = -\left[\ln(\rho)\right]_s f_s \tag{27}$$

where now

$$k_0^2 = \frac{\omega^2}{c_0^2} \tag{28}$$

In order to reduce (27) into a Schrödinger-like equation, we let

$$f = u^{-1/2}\psi\,, \tag{29}$$

where $u \equiv [\ln(\rho)]$, to obtain

$$\psi_{ss} + \left[k_0^2 - V(s)\right]\psi = 0 \tag{30}$$

where the effective potential $V(s)$ in the $s$-space is given by

$$V(s) = \frac{3}{4}\frac{u_s^2}{u^2} - \frac{1}{2}\frac{u_{ss}}{u} \tag{31}$$

which is equivalent to that given in [10], namely,

$$V(s) = \frac{1}{4}\left[(\ln u)_s\right]^2 - \frac{1}{2}(\ln u)_{ss}\,. \tag{32}$$

Equation (30) has the same structure as the Schrödinger equation (1). Therefore, when the potential $V(s)$ is real and non-vanishing for $0 < s < \infty$, the above one-dimensional Marchenko formalism can be applied in a straightforward manner.

## 3 Applications

### 3.1 Quantum Systems

Let us demonstrate first the application of the Marchenko Inversion (MI) method in one-dimensional quantum systems. The purpose of revisiting the problem is threefold. First, to demonstrate the reliability of the method in handling quite complicate potentials that give rise to a reflection coefficient having a considerable resonance structure; second, to expose features of the MI that will be useful in extending the method to classical systems; third, to demonstrate how it can be used to construct profiles with predetermined characteristics. The potential used for this purpose is shown in Fig. 2. This potential can be easily constructed by assuming that $V(x)$ starts at $x_A$ and ends at $x_B$, with $L = x_B - x_A$ while the maximum value of it at $x_A$ is

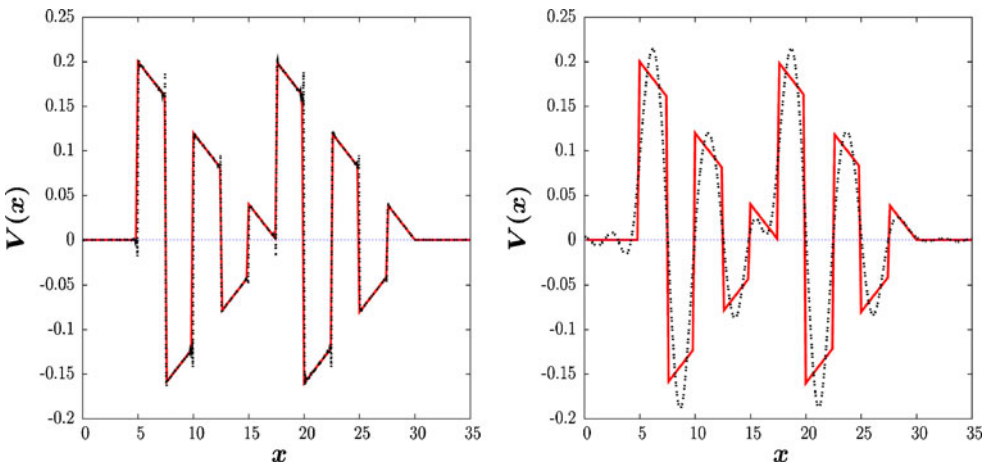


**Fig. 2** The original potential (*solid line*) and its reproduction (*dotted line*) by the MI method (*left*). The omission of the high momentum part of $R(k)$ results in a potential with rounded edges (*right*)

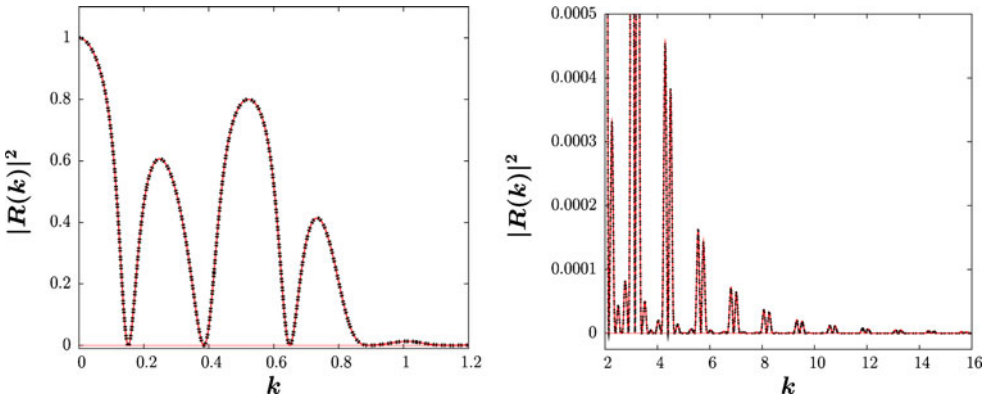


**Fig. 3** The low (*left*) and high (*right*) momentum reflectivity generated by the original and the inversion profiles shown in Fig. 2. *Dotted lines* correspond to reflectivities obtained by inversion

$V_0$. If the width of each oscillation is $d$ then the left part of the potential shown in Fig. 2 is given by

$$V(x) = \begin{cases} 0 & x > x_B \\ (-1)^n \dfrac{V_0}{L}(x_B - x) & x_A + id \le x < x_A + (i+1)d, \\ & i = 0, 1, \cdots, \mathrm{int}(L/d) \\ & n = \mathrm{mod}(i, 2) \end{cases} \tag{33}$$

Similarly, one constructs the right branch of the potential. Using this potential, we generated the reflection coefficient $R(k)$ for $k \in (0, k_{\max})$ which when used as input in (7) provided us the Fourier transformation $B(x)$ needed to obtain the solution of the Marchenko equation.

For $k_{\max} = 16$, the reflectivity becomes practically zero and the reproduction by inversion is perfect except that there appear small spikes at the sharp edges due to numerical inaccuracies in obtaining the derivative, (9), for the extraction of the potential. Such a zig-zag potential is expected to generate strong resonance behavior at low as well at high energies. This behavior is shown in Fig. 3. The high-energy behavior is of particular interest as even at incident energies much higher than the profile, the quantum effects are quite strong and generate considerable spells of interference patterns. The use of $R(k)$ at such high momenta is crucial in the inversion procedure and their omission results in a potential with rounded edges as shown in Fig. 2, right.

In practice, the inversion procedure is difficult to apply in practical problems due to the aforementioned "phase problem" and by the requirement that the $R(k)$ must be known at all incident momenta. However, the inversion can be usefully applied to provide us structures with specific predetermined characteristics as discussed in [9]. For example, in order to generate a filter which removes the second reflectivity peak shown in Fig. 3, i.e., by demanding that $|R(k)| = 0$ in the region $k \in (0.384, 0.650)$, we use the healing conditions for zero reflectivity that ensure continuity in $R(k)$ and the new Fourier transformation (12). This results in the new potential shown in Fig. 4 (left) that generates an

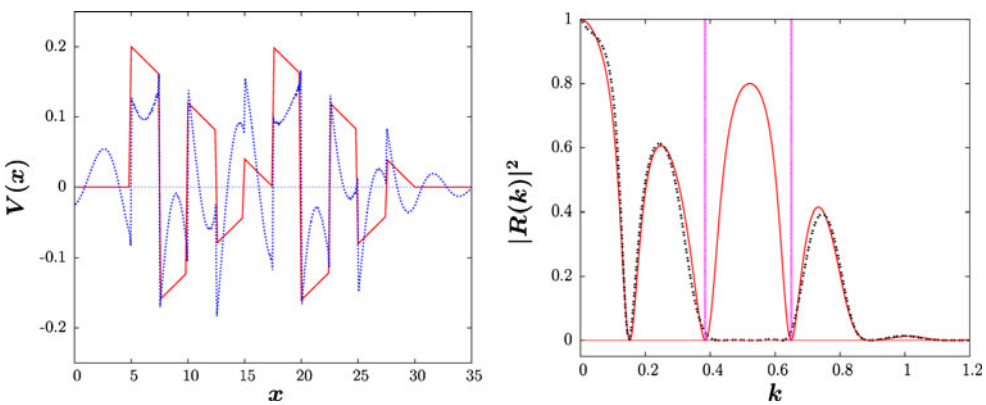


**Fig. 4** The modified potential (*left graph*) generating the new reflectivity (*right graph*) that exhibits zero values in the region $k \in (0.384, 0.65)$ indicated by the *vertical lines*

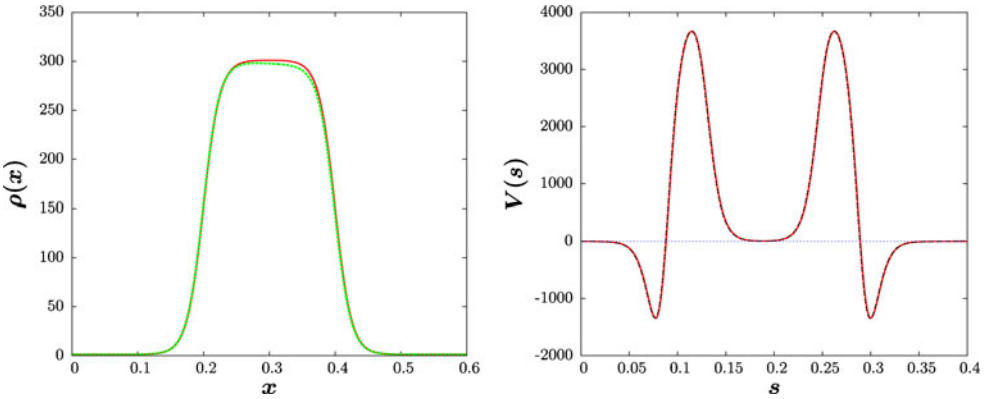


**Fig. 5** The $\rho(x)$ (*left*) and the resulting effective potential $V(s)$ (*right*) and their reproduction by inversion (*dotted lines*)

$|R(k)|$ which has, to all practical purposes, zero values in the prescribed region indicated by the two vertical lines. This is shown in Fig. 4 (right).

### 3.2 Acoustics

The implementation of the MI method in classical systems can be achieved in three steps: Transformation into the $s$-space, (25), construction of $\rho(s)$, and thus of $V(s)$, (31), which is then used to extract the reflection coefficient $R(k)$, (8), and finally obtaining the solution of Marchenko equation for $M(s, s')$. Once the inversion potential is obtained we may use (32) to reconstruct the corresponding $\rho(s)$ which can be transformed into the $x$-space and compared with the original density.

As a first example, we consider acoustic waves traveling with speed $c_0 = 343\,\text{m/s}$ in air of density $\rho_0 = 1.225\ \text{kg/m}^3$ and falling onto a stone wall of thickness $d = 0.2$ m and of density $\rho_1 = 300\ \text{kg/m}^3$ as shown in Fig. 1. As can be seen in (31), for the one-dimensional case the effective potential depends only on the shape and extend of the density and it partially reflects or transmits the waves with speed $c_1 = 5{,}971$ m/s.

In applying our method, we may consider a perfectly square barrier to represent the profile. However, this results in two problems. The first is that the resulting potential has extremely sharp edges that give a reflection coefficients $R(k)$ which diminishes at very large values of $k$ and thus one has huge numerical problems in obtaining accurately the Fourier transformation. The second problem is in the construction of the effective potential which requires derivatives at the edges of the profile and thus any sharp spike in the potential makes the solution of the Marchenko equation cumbersome and unstable. To avoid this, we assume that the speed of sound and the impedance $Z = \rho c$ change in the whole $s$-space region in a smooth way according to

$$c(s) = c_0 F(s) + c_0 \tag{34}$$

$$Z(s) = Z_1 F(s) + \rho_0 c_0 \tag{35}$$

where the function $F(s)$ is chosen to be

$$F(s) = \frac{1}{1 + \exp\left[(s_1 - s)/a_1\right]} - \frac{1}{1 + \exp\left[(s_2 - s)/a_2\right]} \tag{36}$$

where the diffuseness parameters $a_i$, $i = 1, 2$, control the smoothness at the edges of the profile: smaller

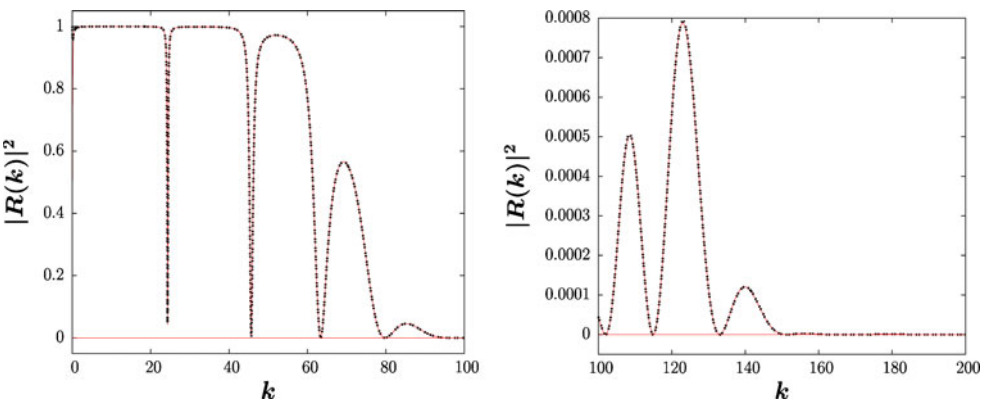


**Fig. 6** The low (*left*) and high momentum (*right*) behavior of the reflectivity and its reproduction by inversion

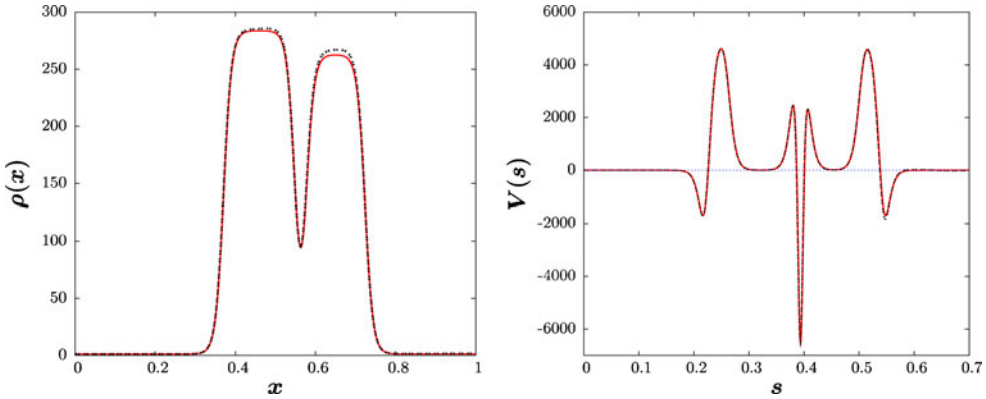


**Fig. 7** The $\rho(x)$ (*left*) and the resulting effective potential $V(s)$ (*right*) and their reproduction by inversion (*dotted line*)

values of $a_i$, (for example 0.001) give rise to sharp edges and the resulting potential has spikes while larger values (for example 1.0) give a rounded smooth edge. Values of $a_i \sim 0.03$ results to reasonably smooth edges in the effective potential. This approximation also affects $R(k)$ which for large values of $a_i$ becomes more transparent, i.e., it is going to zero quite fast and therefore the evaluation of the Fourier transformation, (7), is easier.

In the present example, the underlying density $\rho(x)$ (obtained with $a_i = 0.0125$) is shown in Fig. 5 (left) together with the input effective potential $V(s)$ (right). The dotted lines indicate the reproduction of them after the implementation of the MI. The corresponding reflection coefficient for $k \in (0, 400)$ is shown in Fig. 6. Although the reflectivity $|R(k)|^2$ becomes very small beyond $k = 200$ (practically zero), the inclusion of $R(k)$ values of up to ~350 is necessary as the real and imaginary part of $R(k)$ in this region still contributes to the evaluation of the Fourier transformation $B(x)$, (7). The difference to the quantum case at high energies should be noted: While in the quantum case one has strong interference patterns, in the classical case the interference patterns are weak and diminish fast.

Several cases of inversion for a three-layer medium were considered with various materials. The results were similar to the above which demonstrate the applicability of the MI procedure in acoustics in these simple systems.

We turn now our attention to the more demanding five-layer medium in which two profiles are next to each other, i.e., we have a system air/profile 1/air/profile 2/air. As an example, we choose a stone of thickness $d = 0.12\,\text{m}$, $c = 5{,}971$ m/s and $\rho = 300$ kg/m$^3$ and a wood of thickness $d = 0.1\,\text{m}$, $c = 3{,}300$ m/s, and $\rho = 290$ kg/m$^3$. The diffuseness parameter was chosen to be $a = 0.01$. In Fig. 7, we present the input $\rho(x)$ and effective potential $V(s)$ together with their reproduction by inversion. The corresponding reflectivities and their reproduction at low and high momenta are shown in Fig. 8.

The shape of the effective potential $V(s)$ and of the resulting resonance behavior of the reflection coefficient depends strongly on the distance between the two materials considered and the value of the diffuseness parameter. This is demonstrated in another five-layer example, shown in Fig. 9, consisting of stone and wood of thickness 0.1 and 0.05 m the diffuseness

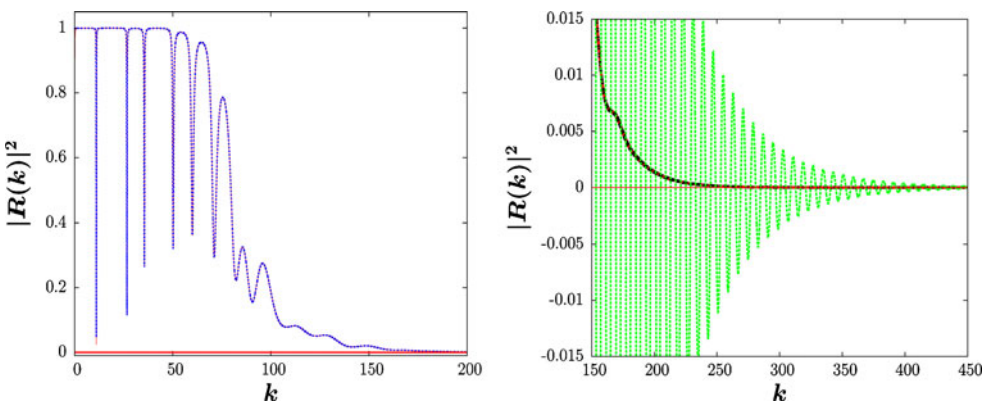


**Fig. 8** The reflectivity (*left*) and its comparison with the real part of $R(k)$ at high momenta (*right*) for the potential shown in Fig. 7. The reproduction of the reflectivity by inversion is also shown (*dotted lines*)

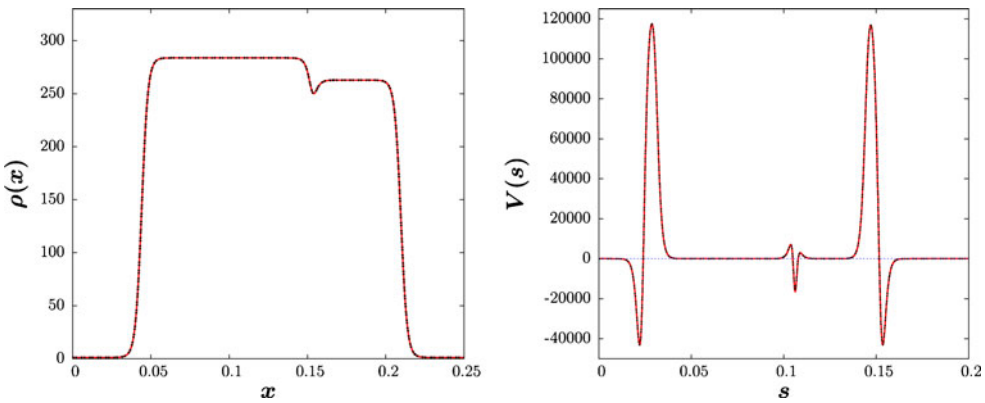


**Fig. 9** The $\rho(x)$ (*left*) and the resulting effective potential $V(s)$ (*right*) and their reproduction by inversion (*dotted line*)

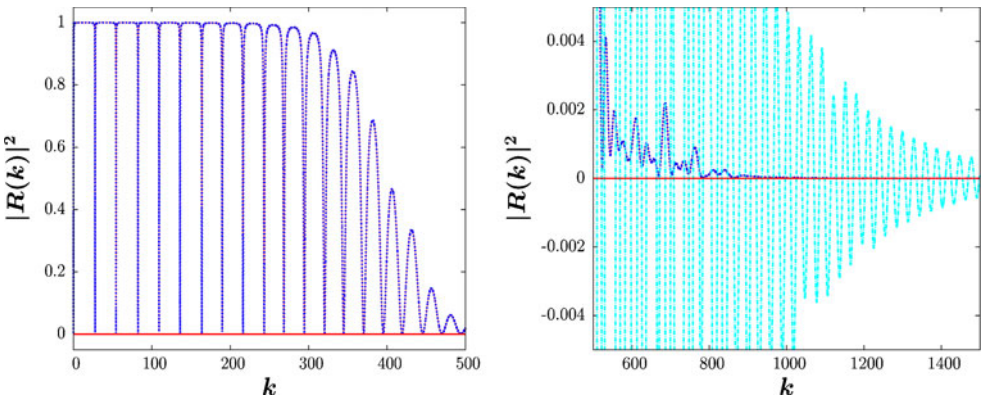


**Fig. 10** The reflectivity and the real part of the reflection coefficient for the potential shown in Fig. 9 and their reproduction by inversion

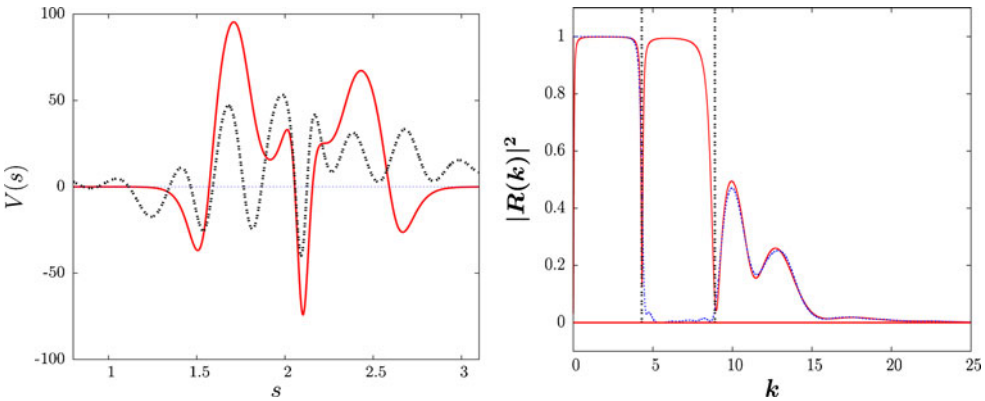


**Fig. 11** The five-layer profile (*left*) and the corresponding reflectivity (*right*), *solid lines*. The modified profile and the generated desired reflectivity $|R(k)|^2 = 0$ within $k \in (3.3, 8.9)$ are shown with *dotted lines*

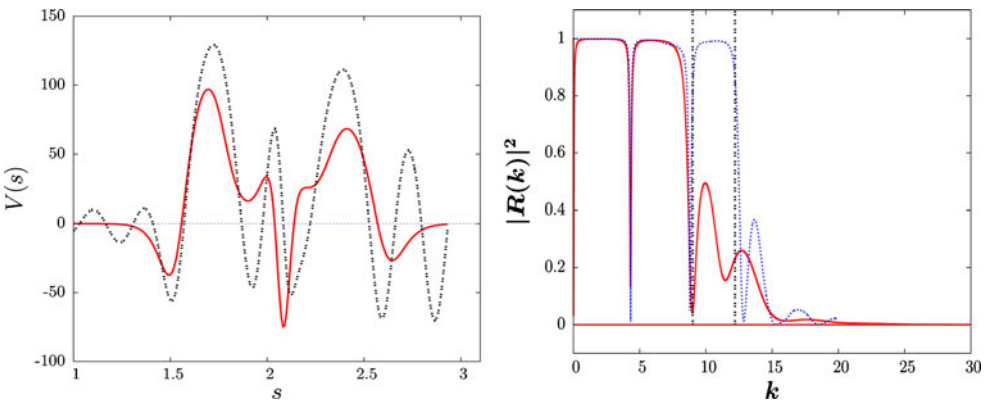


**Fig. 12** Same as in Fig. 11 but with a reflectivity $|R(k)|^2 = 1$ within $k \in (9.0, 12.2)$

parameter being 0.002. The small diffuseness parameter generates sharp edges in the potential which has positive values close to 120,000 as compared with the previous potential which are of the order of 4,000. This results to a lot of resonances in the reflection coefficient $R(k)$ which goes to zero at very high momenta. This is shown in Fig. 10.

It is seen that although the $|R(k)|^2$ becomes practically zero around $k = 800$, the real (and imaginary) part of $R(k)$ becomes insignificant only beyond $k = 1{,}500$. Once again we stress that the inclusion of the high momentum part of $R(k)$ is essential in obtaining all relevant physical quantities which then coincide, to all practical purposes, with the original ones.

Let us turn now our attention to the possibility of constructing a profile having a desired reflection and transmission properties. As an example, we consider the five-layer profile consisting of air–stone–air–wood–air, shown in Fig. 11 (left), generating a reflectivity shown in the same figure (right). By requiring that the reflectivity is zero in the region $k \in (3.3, 8.9)$, we obtain a profile shown in Fig. 11 (left, dotted line). We see that in order to achieve the required zero window, we need an effective potential $V(s)$ which in both left and right regions is oscillatory. Similarly, by requiring that the reflectivity is one in the region $(9.0, 12.2)$, we obtain the results shown in Fig. 12. We notice that the required profile also has an oscillatory structure. The small differences between the original and modified reflectivity for $k > 8.9$ is due to the cut-off of the potential for $s > 3$.

## 4 Conclusions

We considered the Marchenko inverse scattering procedure in one-dimension for systems that obey the Schrödinger or Schrödinger-like wave equation. The inversion problem for quantum systems is first revisited in order to expose the characteristics of the procedure in systems in which the reflectivity has a strong resonance structure and, furthermore, to demonstrate how the ISP can be usefully applied to construct profiles with predetermined reflection and transmission properties. This knowledge could be very useful in applications of the ISP to classical systems which in our case consist of one-dimensional profiles reflecting acoustic plane waves. It was found that the application of the ISP in quantum profiles with considerable structure can be easily implemented and therefore the construction of devices with predetermined properties, as described in details in [9], is possible and that the method can be extended to classical systems as well.

As far as classical systems are concerned, one has to transform first the classical wave equation from the one-dimensional $x$-space to the $s$-space defined by (25). This enable us to reduce it to a Schrödinger-like equation in which the effective potential $V(s)$ depends on the shape and extension of the underlying density $\rho(s)$. When the potential is smooth and bounded, the Schrödinger-like differential equation can be brought into the Marchenko integral equation for the nonlocal function $M(s, s')$ in the transformed $s$-space. The latter depends only on the Fourier transform of the reflection coefficient $R(k)$ corresponding to the effective potential $V(s)$.

In implementing the classical ISP, we found that the numerical and physical experiences gained in quantum systems can be taken over to classical systems in a straightforward manner. One such experience is that a good inversion requires that the reflection coefficient is known at all momenta $k \in (0, k_{\max})$ where the $k_{\max}$ is such that both the real and imaginary parts of $R(k)$ become practically zero. Then the Fourier transformation provides us with the full information needed to obtain the function $M(s, s')$ accurately and thus to extract the underlying effective potential $V(s)$ and hence the original density $\rho(x)$ of the profile.

It should be emphasized here that in the Acoustic case one has to assume that in moving from one medium to another there is a smooth transition. Sharp changes of the density $\rho(x)$ and of the other relevant quantities in moving from one medium to the next, results to effective interactions which have spikes that give rise to numerical instabilities. Furthermore, the $k_{\max}$ becomes huge and thus further numerical problems arise (especially in calculating the Fourier transformation, (7)). Therefore, the inversion procedure becomes hugely cumbersome. The smooth transition from one medium to another may be physical and in fact it can be used to generate a reflection coefficient with desirable characteristics.

The extraction of the reflection coefficient $R(k)$ for the underlying profiles could be by itself very useful as it reveals the reflection properties of the system. Furthermore, it can be used as an input to implement the MI method. The excellent results obtained with the MI for classical systems in all cases tested, demonstrate that the method could indeed be very useful in practical applications as well. This has been demonstrated by assuming that the reflectivity is zero or one within a certain energy region. More work, however, is required to fully understand the dynamics of the inverse scattering in acoustics with the MI scheme. This includes the handling of standing waves, the blocking or channeling through of waves at certain momenta through easily

constructible profile(s), and, most importantly, the role played by the thickness and the distance between the profiles and their shapes.

**Acknowledgement** This work was supported by the Greek General Secretariat for Research and Technology, innovation voucher 67107608–01–000171.

## References

1. Z. S. Agranovich, V. A. Marchenko, *The Inverse Problem of Scattering Theory* (Gordon & Breach, New York, 1963)
2. K. Chadan, P. C. Sabatier, *Inverse Problems in Quantum Scattering Theory*, 2nd edn. (Springer, New York, 1989)
3. D. N. Ghosh Roy, *Methods of Inverse Problems in Physics* (CRC Press, Boston, 1991)
4. D. Coldon, R. Kress, *Inverse Acoustic and Electromagnetic Scattering Theory* (Springer, New York, 1991)
5. H. Lipperheide, G. Reiss, H. Fiedeldey, S. A. Sofianos, H. Leeb, Physica **B 190**, 377 (1993)
6. M. Braun, S. A. Sofianos, R. Lipperheide, Inverse Probl. **11**, L1 (1995)
7. C. V. Sukumar, J. Phys. A: Math. Gen. **18**, L57 (1985); **18**, 2917 (1985); J. Phys. A: Math. Gen. **18**, 2937 (1985)
8. M. Braun, S. A. Sofianos, H. Leeb, Phys. Rev. A **68**, 012719 (2003)
9. S. A. Sofianos, G. J. Rampho, H. Azemtsa Donfack, I. E. Lagaris, H. Leeb, Microelectron. J. **38**, 235 (2007)
10. B-Q. Xu, N. Ida, Int. J. Appl. Electromagn. Mech. **2**, 39 (1991)